Acta Geophys. (2017) 65:119–138
DOI 10.1007/s11600-017-0011-3

RESEARCH ARTICLE

Magnetic investigation and 2½ D gravity profile modelling across the Beattie magnetic anomaly in the southeastern Karoo Basin, South Africa

Christopher Baiyegunhi[1] · **Oswald Gwavava**[1]

Received: 17 January 2017 / Accepted: 20 January 2017 / Published online: 1 February 2017

Abstract The southeastern Karoo Basin is considered to be one of the most prospective areas for shale gas exploration in South Africa. An interesting magnetic anomaly, the Beattie magnetic anomaly (BMA), and geologic intrusions are seen on the magnetic map. To date, the source of the BMA and interconnectivity of the igneous intrusions are not well understood. In this study, we investigate the interconnectivity of the igneous intrusions and possible location of the source of the BMA using gravity and magnetic methods. The gravity model results showed that igneous intrusions are interconnected at depth, which probably pose threat by increasing the risk of fracking the Karoo for shale gas exploration. The magnetic results revealed that the BMA becomes stronger with depth. The average depths to the top of the shallow and deep magnetic sources were estimated to be approximately 0.6 and 15 km, respectively.

Keywords Magnetic anomaly · Igneous intrusions · Gravity · Models · Karoo Basin

Introduction

Two distinctive geophysical anomalies, the Beattie magnetic anomaly (BMA) (Beattie 1909) and the Southern Cape Conductive Belt (SCCB) (De Beer et al. 1982) cut across the southeastern Karoo Basin. The BMA is the largest known magnetic anomaly in the southern Karoo Basin; it was first discovered by Beattie (1909) and later documented by several researchers like Gough et al. (1973), Pitts et al. (1992), Weckmann et al. (2007a, b), Lindeque et al. (2007), and Stankiewicz et al. (2007). A regional aeromagnetic survey conducted by Fugro Airborne Surveys in 1972 over the Eastern Cape Province of South Africa also picked up this set of anomalies that possibly extend into Antarctica and southern South America. The magnitude of the anomaly ranges from about 200–500 nT, thus making it one of the world's largest magnetic anomalies (Weckmann et al. 2007a). The result of the geo-electrical and gravity geophysical investigation of the BMA by De Beer and Meyer (1983, 1984) revealed that the anomaly marks the southern boundary of the Namaqua–Natal Mobile Belt (NNMB). It is confined to the continental crust (Du Plessis and Simpson 1974). The upper and lower boundaries of the anomaly are due to two crustal discontinuities in the region that were identified at depths of about 7–11 and 17–19 km, respectively (Harvey et al. 2001).

The BMA spatially coincides with the central part of the 100–200 km wide electrically conductive zone known as the SCCB (Gough et al. 1973; Lindeque et al. 2007). They suggested that the BMA and SCCB have a common source and that the conductive material that trends east–west beneath the southern Karoo Basin and Cape Fold Belt lies in the crust. Both the BMA and SCCB anomalies are parallel to the tectonic edge or margin of the NNMB and the Cape Fold Belt (CFB). Harvey et al. (2001) and Lindeque et al. (2007) documented that the tectonic structures resulted from the continual addition or deposition of sediments over time. Schreiber-Enslin et al. (2013) also emphasized the importance of understanding the source of the BMA to ascertain or create a precise potential model of

✉ Christopher Baiyegunhi
201201530@ufh.ac.za; cbaiyegunhi@yahoo.com

[1] Department of Geology, Faculty of Science and Agriculture, University of Fort Hare, Alice, Eastern Cape Province, South Africa

the Karoo Basin and to know the evolutionary history of the Karoo Basin. With the use of Curie isotherm calculations, De Beer and Gough (1980) suggested that the BMA is possibly due to a source at about 25–38 km depth. Pitts et al. (1992) proposed that the BMA may be due to a magnetic body that extends from depths of 7–30 km and infer that serpentinised oceanic crust could be the source of the BMA. A recent magnetotelluric survey shows no indication or sign for such a body (Weckmann et al. 2007a).

Geophysical surveys (i.e., geo-electrical and gravity (De Beer and Meyer 1983), seismic reflection (Hälbich 1983; Hälbich 1993), near vertical seismic (Lindeque et al. 2007) and magnetotelluric (Weckmann et al. 2007a, b) across the western part of the BMA shows an anomaly source depth of 10–15 km within the mid-crust. It was earlier assumed that the BMA is due to the partially serpentinised oceanic lithosphere probably connected to a suture zone. However, Lindeque et al. (2011) as well as Schreiber-Enslin et al. (2013) suggested that the BMA is part of the tectono-metamorphic NNMB and associated shear zones. To date, due to insufficient geophysical information, the precise location of the source as well as the possible source for the BMA is still debatable. In this paper, we present the result of magnetic derivatives, power spectrum, depth slicing and simple gravity profile models that revealed the configuration of the basin and how geologic structures, such as dolerite sills and dykes, are interconnected at depth. In addition, we critically examined the gravity models to see any possible anomalous features that can be inferred to be caused by the BMA and SCCB sources.

Geological setting

The main Karoo Basin in South Africa covers up to 700,000 km^2 and represents about 100 Ma of sedimentation spanning from 280 to 180 Ma (Johnson et al. 2006). The deposition of Karoo sedimentary rocks that cover almost two-third of the area of South Africa occurred during the Late Carboniferous across the Gondwana, and span until the breakup of the Gondwana supercontinent during the Middle Jurassic (Catuneanu et al. 1998; Geel et al. 2013). The Karoo Basin is believed to have evolved from two distinct tectonic regimes sourced from the southern and the northern margin of Gondwana (Catuneanu et al. 1998, 2005). The southern tectonic regimes are believed to be related to the processes of subduction and orogenesis along the Panthalassan (paleo-Pacific) margin of Gondwana. In addition, it resulted in the formation of a retro-arc foreland system known as the "main Karoo Basin" in association with the primary subsidence mechanism represented by flexural and dynamic loading. The northern event was associated with extensional stresses that propagated southwards into the supercontinent from the divergent Tethyan margin of Gondwana. Superimposed on the tectonic control on basin development, climate fluctuations also left a mark on the stratigraphic record. In addition, it shows evidence of a general shift from cold and semi-arid conditions during the Late Carboniferous—Earliest Permian interval, to warmer and eventually hot climates with fluctuating precipitation during the rest of the Karoo time (Keyser 1996 in Catuneanu et al. 2005).

The importance of the tectonic control on Karoo Basin development and sedimentation was first proposed by Rust (1973) and subsequently modified by several researchers (i.e., Tankard et al. 1982; Smith et al. 1993; Veevers et al. 1994; Johnson et al. 1996). However, Visser (1987) and Catuneanu et al. (1998, 2002, 2005) suggested the evolution of the retro-arc foreland Karoo Basin in relation to fold-thrust belt inboard of magmatic arc. Several authors like De Wit and Ransome (1992), Veevers et al. (1994), Visser (1995) and Catuneanu et al. (1998) envisaged that the Karoo Basin is a retro-arc foreland basin. However, Tankard et al. (2009) gave an alternative interpretation for the tectono-sedimentary evolution of the Karoo Basin by dividing it into a pre-foreland phase and a foreland phase. The Cape Supergroup (Cape basin) spans from the Early Ordovician to Early Carboniferous (Veevers et al. 1994), and consists of up to 8 km of shallow marine, deltaic and fluvial deposits that thicken southwards into an east–west trending depo-axis (Rust 1973; Turner 1999).

According to Tankard et al. (1982), these sediments were believed to have been derived from a cratonic source to the north. The overlying Karoo Supergroup (Karoo Basin) that spans from the Late Carboniferous to Early Jurassic period and consists of about 12 km of deep marine to fluvial deposits. Visser and Praekelt (1996) documented that the Karoo-Falklands basin, the Sierra Australise Colorado basins (Argentina), as well as the Central Antarctic Mountains basin were developed as extensional back-arc basins, in relation to the oblique subduction of the paleo-Pacific plate beneath the western Gondwana. Several major strike-slip systems begin to develop, with the Southern Trans-African Shear system, within the Damara mobile belt. According to Stollhofen et al. (2000), all the Karoo basins in southern Africa can be attributed to the extensional intra-cratonic rifts, in relation to the N–S trending basement shear zones. The detailed record for southern Africa is still less complete when compared to South America and Antarctica, as a result of the major Mesozoic regional strike-slip and extensional tectonics that removed most of the late Palaeozoic record to the south of the present day South Africa (Flint et al. 2011).

Structural elements/features, such as lineaments, faults and intrusions, are present in the study area, as depicted in Fig. 1. Chevallier and Woodford (1999) allude that the

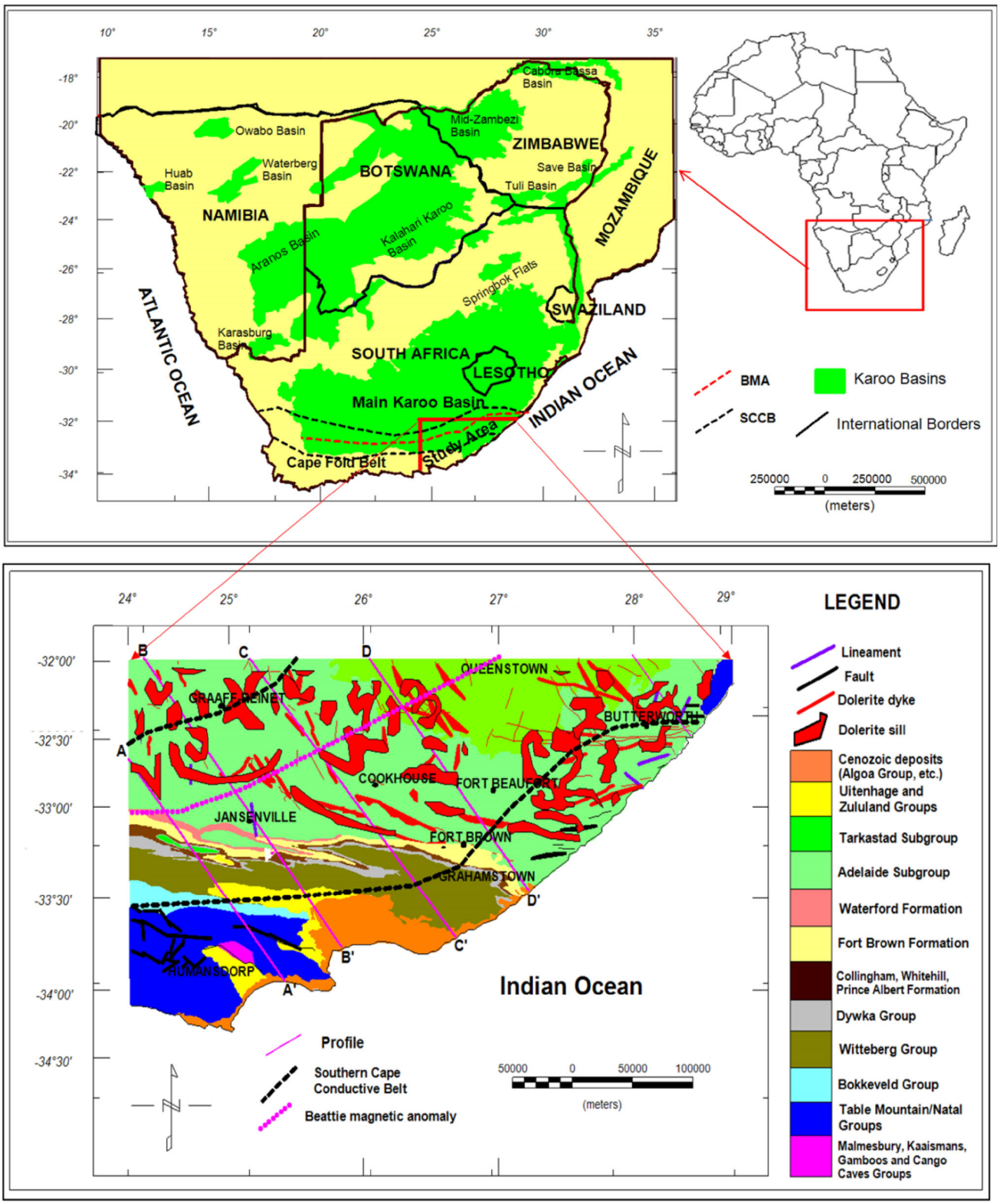

Fig. 1 Geological map of the study area. The map also shows dolerite intrusions (sills and dykes), faults, part of the BMA and SCCB (after Council for Geoscience 1995)

Karoo dolerite, which comprises several petrological facies (ranging from a leucogabbro to a dolerite-pegmatite), consists of interconnected networks of dykes and sills and it is very difficult to single out any particular intrusive or tectonic event due to the fact that, an individual sill can be fed by many dykes of different orientations or a dyke can act as a feeder to two different sills or more. Chevallier and Woodford (1999) and Svensen et al. (2007) concluded that during the intrusive phases, the molten magma concurrently filled in the numerous fractures, and that the dolerite intrusive network probably behaved as a shallow stockwork-like reservoir or storage system where molten magma of different viscosities intruded the fractures. It appears that there is a lithological control on the emplacement of dykes within the Western Karoo Basin, as the bulk of the dykes are strata bound and concentrated in the Upper Ecca and Beaufort Group (Woodford and Chevallier 2002). According to Chevallier et al. (2001), three major structural domains that are indicated by dyke distribution have been identified in the Main Karoo Basin (Fig. 2). These domains are:

- The Western Karoo Domain: It extends from Calvinia to Middelburg and is characterised by two distinctive structural features, east west trending zone of long and thick dykes associated with right lateral shear deformation and north northwest dykes.
- The Eastern Karoo Domain: It extends from Middelburg to East London and comprises two major dyke swarms, namely, a major curvi-linear swarm of extensive and thick dykes diverging from a point offshore of East London and minor north−northeast trending dykes.
- The Transkei–Lesotho-Northern Karoo Domain: It consists of two swarms, northwest trending dykes in the Transkei Region, curving to east–west in the Free State and northeast trending dykes mainly occurring within and alongside the Lesotho basalt.

Stratigraphically, the Karoo Supergroup can be subdivided into five groups, namely, in their ascending stratigraphic order, the Dwyka (Late Carboniferous), Ecca (Early Permian), Beaufort (Late Permian—Middle Triassic), Stormberg (Late Triassic—Early Jurassic), and Drakensberg Groups (Middle Jurassic) (Johnson et al. 2006; Table 1). Johnson et al. (2006) documented that prior to the Middle Jurassic period, the environmental conditions in the Karoo Basin changed rapidly, coupled with the large movement of the Earth's mantle, the crust experienced a large-scale lifting, and eruption of massive volumes of basaltic lava that constitute the Drakensberg Group. The outpourings of the basaltic lava spread across much of Gondwana

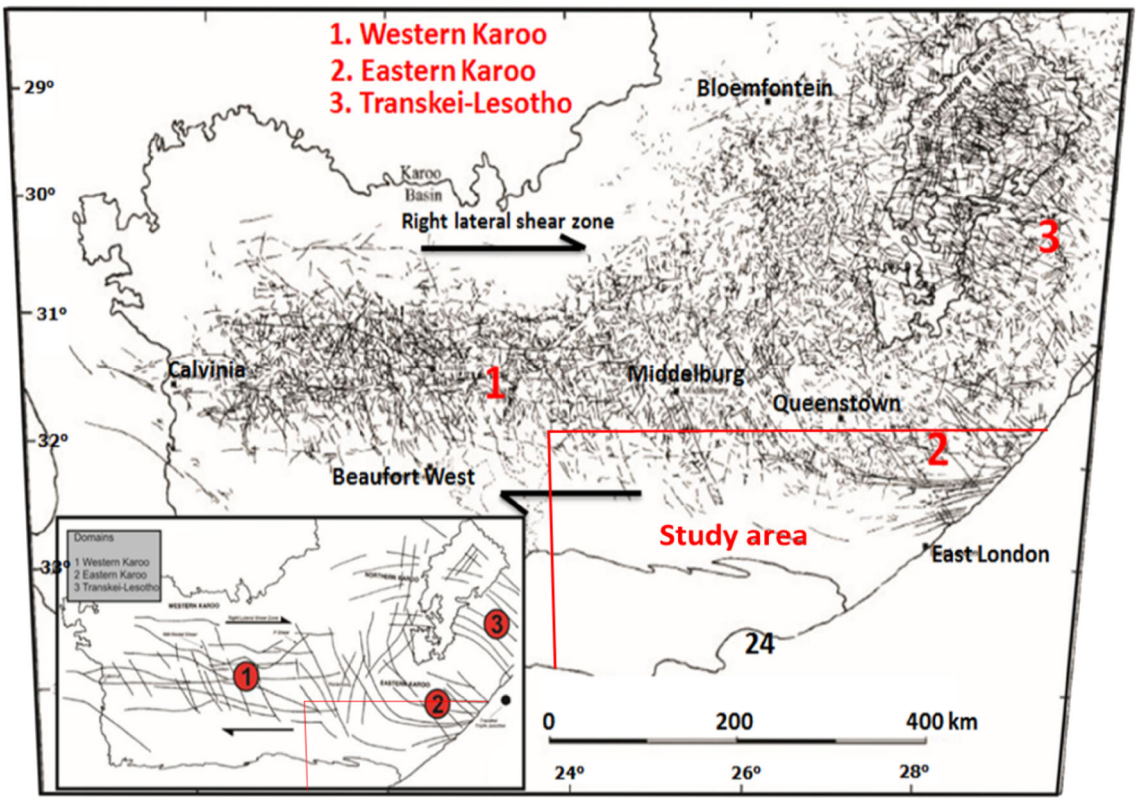

Fig. 2 Dolerite dykes of the main Karoo Basin. *Inset* is a simplified structural map showing the three structural domains (after Woodford and Chevallier 2002)

Table 1 Lithostratigraphy of the Karoo Supergroup in the Eastern Cape Province (Johnson et al. 2006)

Supergroup	Group	Subgroup	Formation	Member	Lithology	Maximum thickness (m)
Karoo			Drakensberg		Basalt	1400
					Pyroclastic deposits	
			Clarens		Sandstone	300
			Elliot		Red mudstone	500
					Sandstone	
			Molteno		Coarse sandstone	450
					Grey and khaki shale	
					Coal seam	
	Beaufort	Tarkastad	Burgersdorp		Red mudstone	1000
					Sandstone light grey sandstone	
					Grey shale	
			Katberg		Light grey sandstone	900
					Red mudstone	
					Grey shale	
		Adelaide	Balfour	Palingkloof	Red mudstone	50
					Light grey sandstone	
				Elandsberg	Sandstone	700
					Siltstone	
				Barberskrans	Light grey sandstone	100
					Khaki shale	
				Daggaboersnek	Grey shale	1200
					Sandstone	
					Siltstone	
				Oudeberg	Light grey sandstone	100
					Khaki shale	
			Middleton		Grey and black shale	1500
					Light grey sandstone	
					Red mudstone	
			Koonap		Grey sandstone shale	1300
	ECCA		Waterford (not present in ECCA Pass)		Sandstone shale	800
			Fort brown		Shale sandstone	1500
			Ripon		Sandstone shale	1000
			Collingham		Grey shale	30
					Yellow claystone	
			Whitehill		Black shale chert	70
			Prince Albert		Khaki shale	120
	DWYKA				Diamicite, tillite, shale	

about 180 million years ago, indicating the start of Gondwana breakup. In this paper, the stratigraphy, geological and tectonic setting of the southeastern Karoo Basin are not reported/documented in detail but can be found in Hälbich (1993), (Hälbich 1983), de Wit and Ransome (1992), Veevers et al. (1994), Visser (1995), Catuneanu et al. (1998, 2002, 2005), Johnson et al. (1996, 2006), De Wit and Horsfield (2006), Tankard et al. (2009, 2012), and Pángaro and Ramos (2012).

Materials and methods

Locations within the Eastern Cape Province where the Karoo Supergroup (Dwyka, Ecca, and Beaufort Groups) (Fig. 1; Table 1) as well as the Cape Supergroup (Table Mountain, Bokkeveld and Witteberg Groups) (see Fig. 1) outcrop were visited for field investigation and sampling. A total of 258 samples were collected on road cut exposures from the geologic formations (Fig. 1) that cover the study area for density measurements.

Determination of dry density

The dry densities of rock samples were obtained from laboratory measurements utilizing the buoyancy determined volume that uses Archimedes' principle. The rock samples were left in the sun for about two weeks, with an average daily temperature of about 25 °C. The samples were dried long enough to remove any moisture from the voids. An average water density value of 1.022 g/cm^3 was obtained and applied when calculating the dry density of the rock samples. The water density values depend on its temperature and pressure, i.e., decrease in temperature results in the water molecules to be well and closely packed together, thereby leading to increase in the density of water and vice versa, but this relationship is not linear. The temperature of water was monitored throughout the experiment and the effect was small or negligible, giving no appreciable change in the density. It could be inferred that the temperature and pressure were fairly constant throughout the experiment period. The dry density of the rocks was calculated from the expression:

$$\rho_{\mathrm{d}} = \left[\frac{\mathrm{d}M_{\mathrm{a}}}{\mathrm{d}M_{\mathrm{a}} - \mathrm{d}M_{\mathrm{b}}}\right] \times \rho_{\mathrm{w}} \quad (1)$$

where ρ_{d} = dry density, $\mathrm{d}M_{\mathrm{a}}$ = mass of dry sample in air, $\mathrm{d}M_{\mathrm{b}}$ = mass of sample in water and ρ_{w} = density of water (determined using a density bottle).

The average density value for each geologic group was obtained from the measured dry density.

Available geophysical data

Aeromagnetic and gravity data in the format of Geosoft files were supplied by Fugro Airborne Surveys and Council for Geoscience, respectively. The supplied magnetic data had all the temporal variation and IGRF removed, to leave the crustal magnetic field. Similarly, the gravity data had been reduced to Bouguer gravity values.

Geophysical data enhancement and filtering

The acquired magnetic original space domain grid was prepared for filtering and enhanced using Geosoft Oasis montaj. The Fast Fourier Transform (FFT) was applied to transform the square and periodic space domain to the wave number domain, and then filters were applied to enhance the effects of shallow magnetic sources (such as removal of first-order trend) or enhance deeper magnetic sources. The inverse FFT was applied, enhancements (i.e., vertical derivative, horizontal derivative, analytical signal and radially averaged spectrum) were calculated, and the results are presented in the form of geophysical maps ("Reduction to the pole (RTP)", "Vertical derivative", "Total horizontal derivative", "Analytical signal", "Power spectrum", sections). Magnetic depth slicing was done using the GETECH GETGRID ("Depth slicing" section). The gridded gravity data was enhanced to specifically remove the first order trend in geosoft. No filtering was carried out on the gravity data; the map is presented in "Gravity" section.

½ D gravity profile modelling

Four profiles (A–D) that are roughly equally spaced to cover the study area were selected (Fig. 1). The geological map of the study area was used to measure the actual profile lengths and positions along the profiles to each geologic group (succession) outcrop within the study area and at infinity (outside the study area but along the profile). This was done to set constraints to the model such that the model will perfectly fit or agree with what is obtained in the real-world. These profiles were modelled and for each profile, 3 models were produced using the minimum, average and maximum density values giving a total of 12 models that were analysed. A starting GM-SYS model was created from a map profile (e.g., A–A′) by importing the gravity grid and elevation grid. The estimated thickness (length) and position of each group from the geological map were used to develop the starting model. Each starting model was extended to infinity at both ends (i.e., a long distance of ±500 km in this case) to eliminate edge effects. The geologic models for the selected profiles were created and real-time calculations of the gravity response of a specific Earth model were performed. The modelling was constrained by the stratigraphic thickness (measured in the field and data from boreholes CR1/68, SP1/69, SC1/67and SC3/67, Table 2), elevation and average density of rocks from various formations of the Karoo Supergroup that outcrop in the study area.

Several authors, like Tedla et al. (2011), Stankiewicz and de Wit (2013) have indicated a Moho depth in the range of 44–50, 40–50, and 40–45 km, respectively, in the study area. To cover the depth envisaged for the Moho by the authors, the depth to the Moho was originally set to vary from about 35 up to 60 km during the modelling process, such that the model will establish the best fit depth for the Moho. The thickness of the modelled dolerite intrusions were estimated from literature (Chevallier and Woodford 1999; Chevallier et al. 2001) and the measured thickness of the intrusions from the boreholes were also used to constrain the models. The modelled dolerite sills and dykes were originally set in horizontal and vertical positions, and allowed to vary during the modelling process to have the best fit model. Since a total of 12 models were

Table 2 Summary of borehole data extracted from Scheiber-Enslin et al. (2014)

Well	Thickness (m)			
	Beaufort group	Ecca group	Dwyka group	Cape supergroup
CR1/68	3600	1700	450	>850
SP1/69	750	1250	70	–
SC1/67	2300	1600	>100	–
SC3/67	1900	1550	45	–

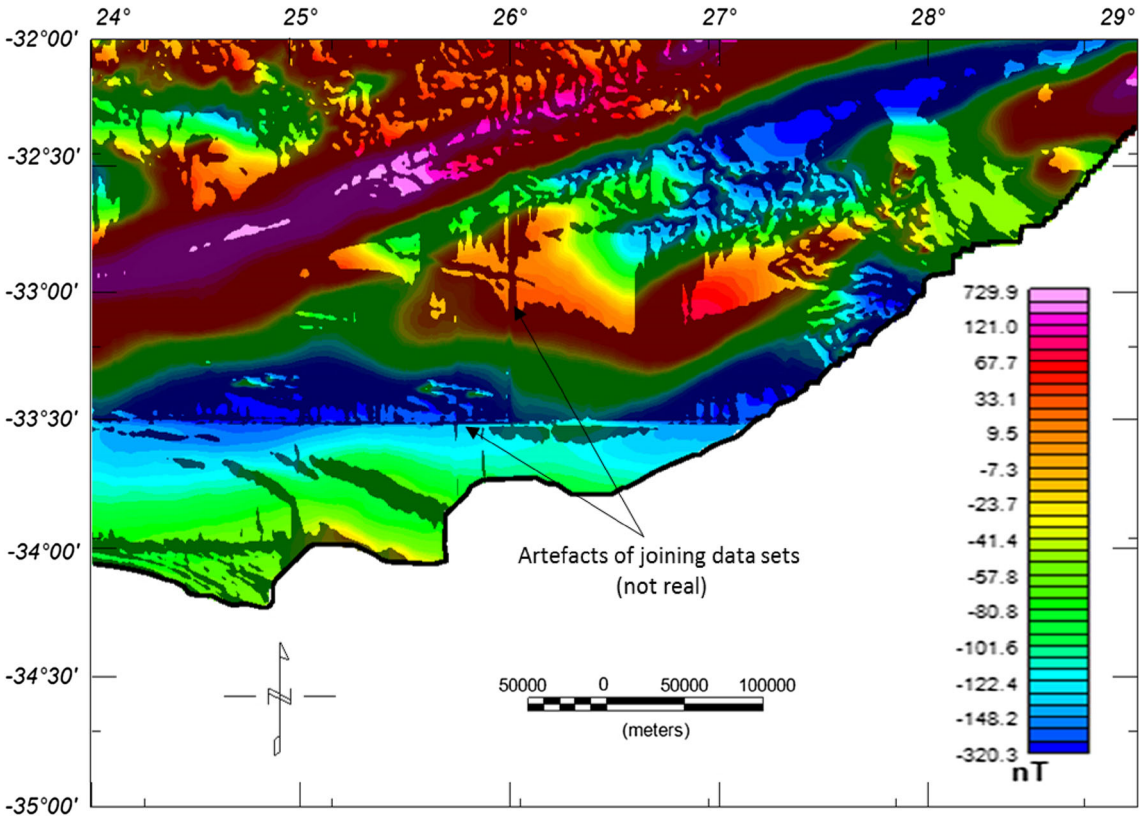

Fig. 3 Reduced to the pole magnetic residual anomaly map

obtained, only those of the average density values are presented in this paper. The alternative models were used to check the sensitivity of the models with respect to change in layer densities and thicknesses.

Results and discussion

Reduction to the pole (RTP)

RTP was performed on magnetic data to remove the asymmetry caused by the inclined main field or convert it to a symmetrical shape (Fig. 3).

The RTP magnetic map (Fig. 3) was overlain on the digitized geological map of the area (Fig. 4) to correlate dolerite intrusions (i.e., dykes and sills) and any other magnetic sources with the magnetic anomalies.

Figure 5 shows three main magnetic anomalies. The first anomaly of up to 729.9 nT extends from west of Jansenville (long. 24°E, lat. 33°S) to north of Fort Beaufort (long. 27°E, lat. 32°S). It is part of the BMA and could be due to a buried body with high magnetic susceptibility minerals. The centre of the first anomaly also shows that the body divides into two, but still trend is in the NE–SW direction. The second anomaly, in the north-eastern part of Butterworth (long. 29°E, lat. 33.5°S) is of relatively small extent with maximum magnetic value of about 227.5 nT. It could be due to dolerite intrusions with associated faulting that are more prominent in the northeastern part of the map. The third anomaly is the "bean shape anomaly" and it coincides with a continuous, regional band of high magnetic susceptibility seen in the centre-eastern part of the map.

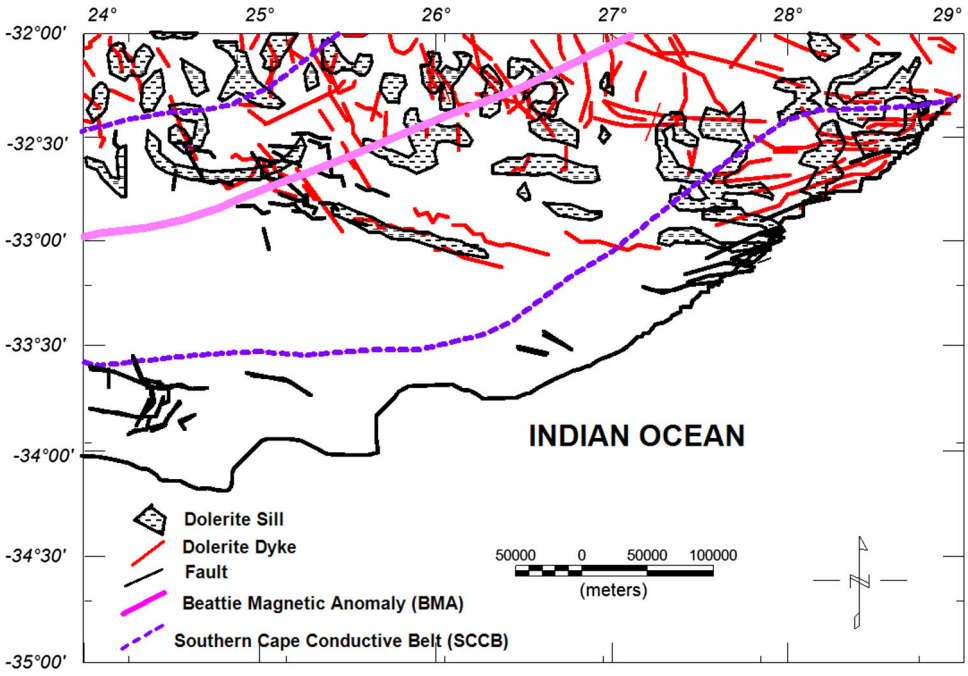

Fig. 4 Digitized geological map of the study area

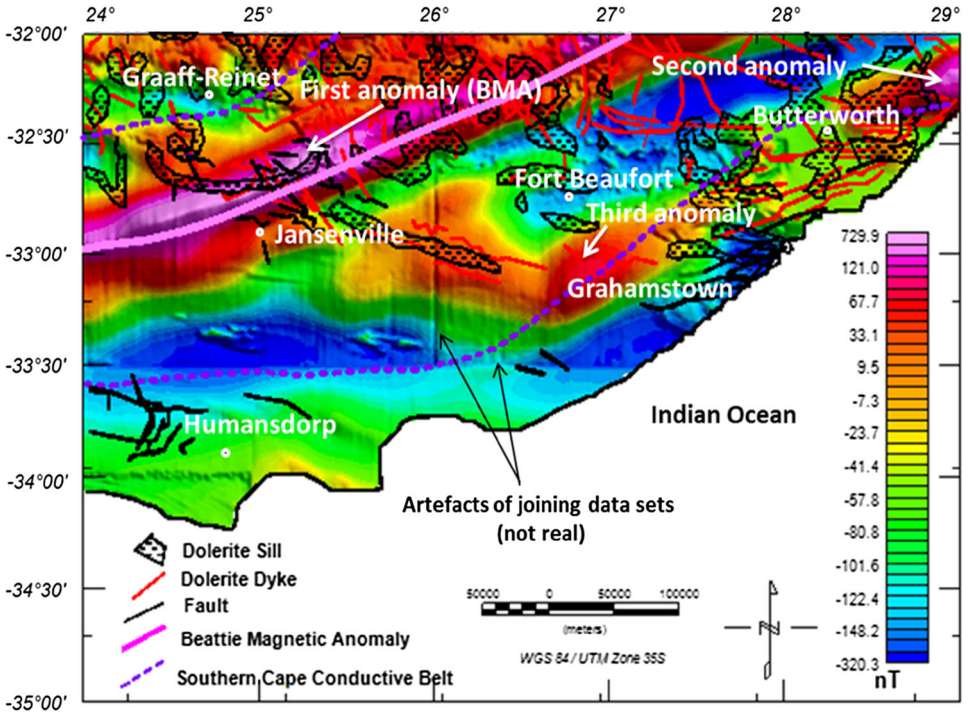

Fig. 5 Reduced to the pole (RTP) magnetic residual anomaly map overlain on the geology

Vertical derivative

The first vertical derivative (Fig. 6) was calculated to enhance the effects of near-surface geology (shallow magnetic sources), suppress anomalies caused by deeper sources, thereby giving a better resolution of closely spaced sources.

The first vertical derivative magnetic map (Fig. 6) was overlain on the digitized geological map (Fig. 4) as depicted in Fig. 7. The splitting of the BMA from long. 25.5°E, lat. 32.5°S to long. 27°E, lat. 32°S is now clearly visible. In addition, the ring structures and linear features due to the dolerite dykes and sills are clear in Fig. 7.

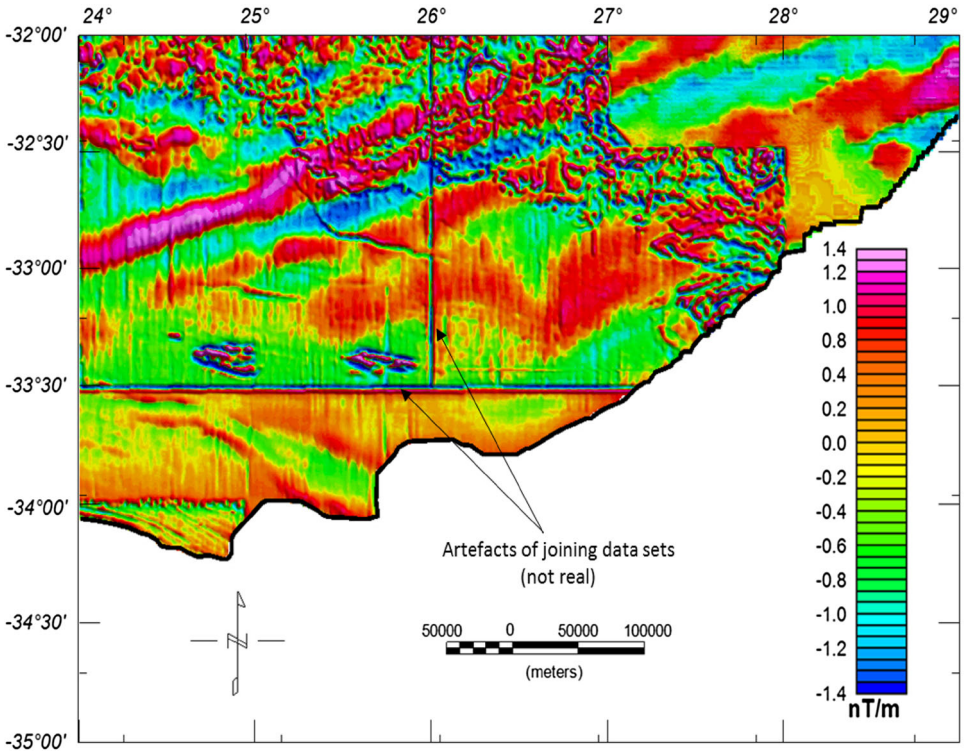

Fig. 6 First vertical derivative magnetic map

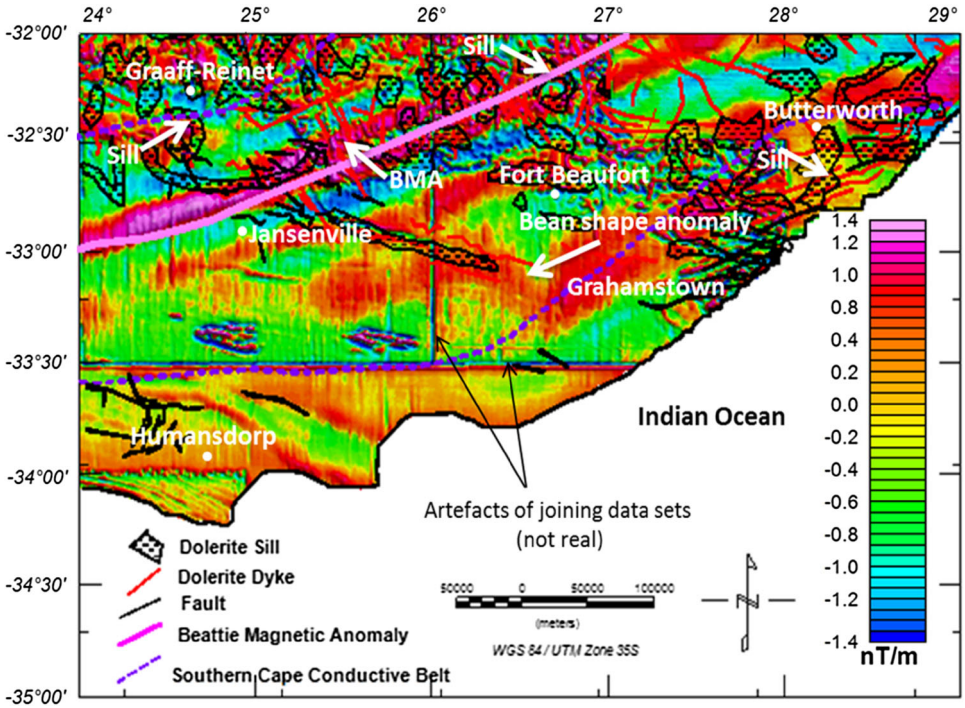

Fig. 7 First vertical derivative magnetic map overlain on the geology

Total horizontal derivative

The first total horizontal derivative of the magnetic field data was calculated in the space domain (Fig. 8). It gives an indication of the boundary structure and this will be accurate for pole reduced data. The first vertical derivative magnetic map (Fig. 8) was also overlain on the digitized geological map (Fig. 4) in order to correlate dolerite intrusions (i.e., dykes and sills) and any other magnetic sources with the magnetic anomalies. The overlain first

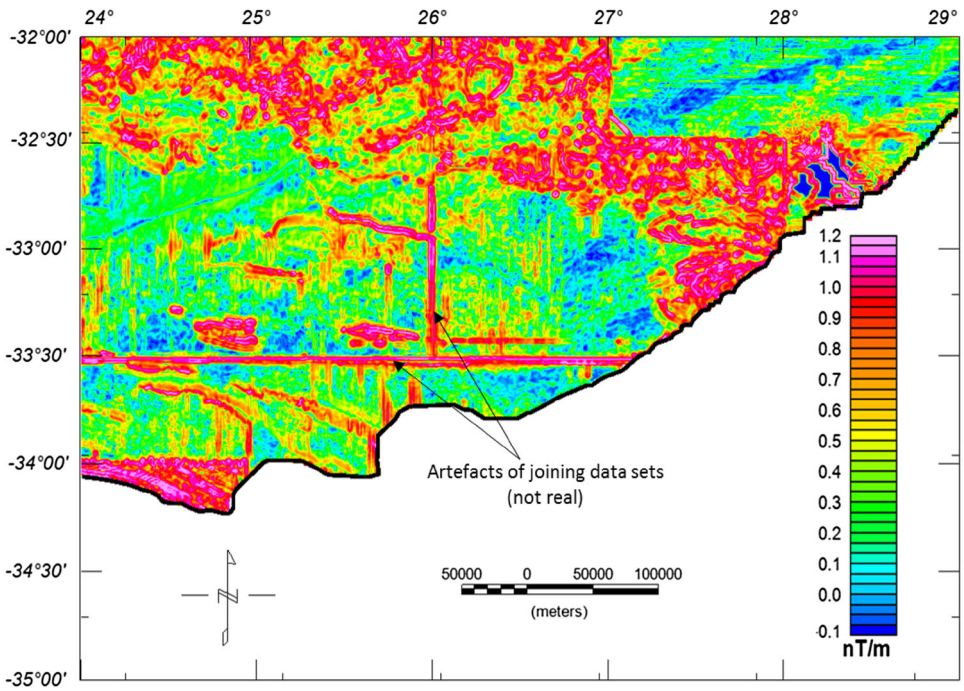

Fig. 8 First total horizontal derivative magnetic map

total horizontal derivative map (Fig. 9) shows interesting ring-like and linear features that extend from north of Graaff-Reinet to the northeastern part of Grahamstown. These features also coincide with the dolerite intrusions on the geological map.

Analytical signal

The analytical signal magnetic map (Fig. 10) was calculated to produce features that are independent of the inclination of the main field and magnetisation direction (either induced or remanent magnetisation direction). This implies that if the geometry of the magnetic sources or bodies is the same, then they will have the same analytical signals. Li (2006) stated that the features produced in 3D case are dependent on the magnetisation direction but when the magnetic source is more than one, the features that are produced on the analytical signal map are effects of shallow sources.

Figure 11 shows highs that clearly outline the BMA, dolerite intrusions and a number of faults. The dolerite intrusions are concentrated in the northern part, while most of the faults are concentrated toward the centre and eastern part (edge) of the map.

Power spectrum

Depth estimation from the spectrum of potential field data (magnetic or gravity) works on the principle that the measured potential field data at the surface is an integral part of the source signature from different depths (Rabeh et al. 2008). The radially averaged power spectrum was calculated in the wavenumber domain and implemented in Geosoft. The radial power spectrum is averagely calculated such that the effect of noise is minimised, ensuring a more accurate result than other commonly used methods (Spector and Grant 1970). The radially averaged power spectrum of the field increases with decrease in depth (h) by a factor that is proportional to exponential ($-4\pi hk$), where k is the wavenumber. Maus and Dimri (1996) stated that, if the depth factor dominates the shape of the power spectrum, then the logarithm of the power spectrum must be proportional to $-4\pi h$. Thus, the slope of the log of the radially averaged spectrum can be used directly to estimate the depth to source.

Quite often, the power spectrum has a linear segment and, for each segment, a depth can be calculated since the slope is $-4\pi h$. Two linear segments can be fitted in Fig. 12 and this corresponds to a depth of 0.6 km (shallow sources) and 15 km (deeper sources).

Depth slicing

Depth slicing entails the use of linear filters to isolate (i.e., based on wavelength criteria) anomaly contributions to a map derived from source bodies in a certain depth range. It creates separate magnetic maps for a sequence of layers at a particular depth, thus allowing the comparison of amplitude response and recognition of the disappearance and arrival of magnetic units at different depth. Depth

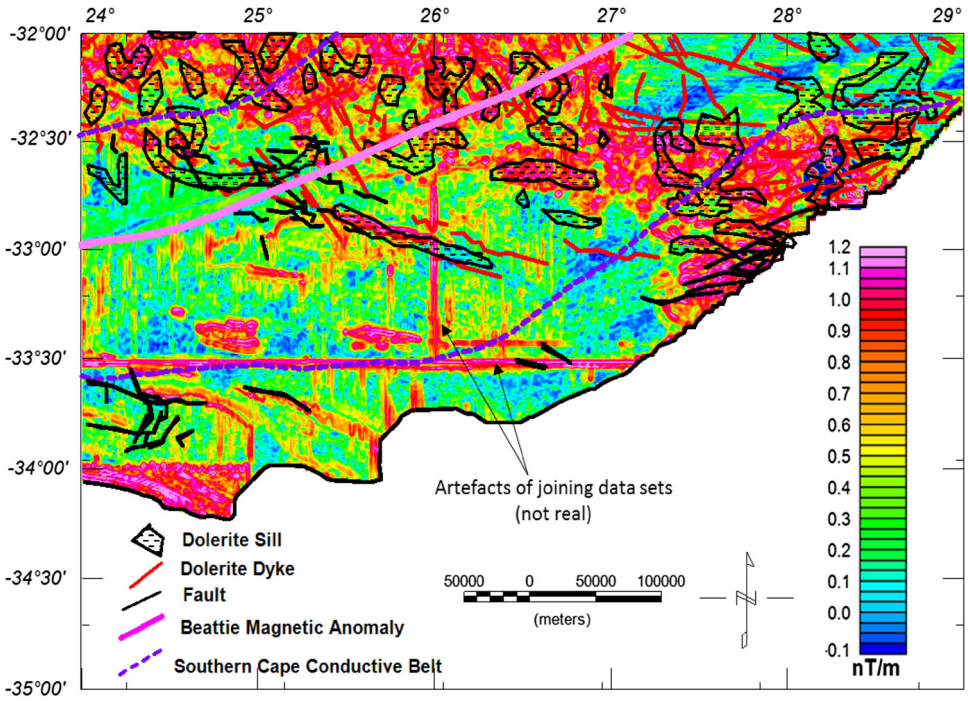

Fig. 9 First total horizontal derivative magnetic map overlain on the geology

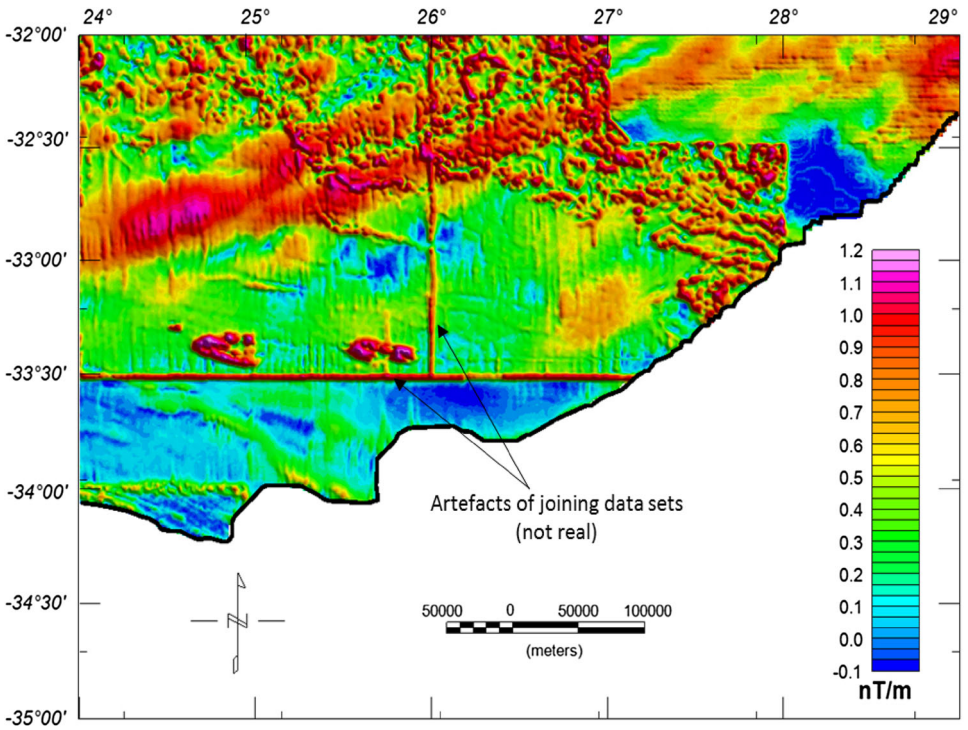

Fig. 10 Analytical signal magnetic map of the study area

slicing works on the principle of Wiener filtering, which assumes that potential field signals (e.g. magnetic and gravity) results from two or more uncorrelated arbitrary processes (Fuller 1967). Fuller (1967) stated that the various components of the data can be separated by highlighting the effects of shallow sources from deeper sources. Most magnetic anomalies at the surface usually originate at a shallow depth, while obscure magnetic anomalies usually originate from a deeper depth (Gunn 1972).

Depth slices (Fig. 13) were used to compare the anomaly amplitude responses at different depths. Thus, anomalous features at a particular depth can be isolated and recognised. Depth slice results (slices 1–3) clearly show structural trends that coincide with dolerite intrusions on

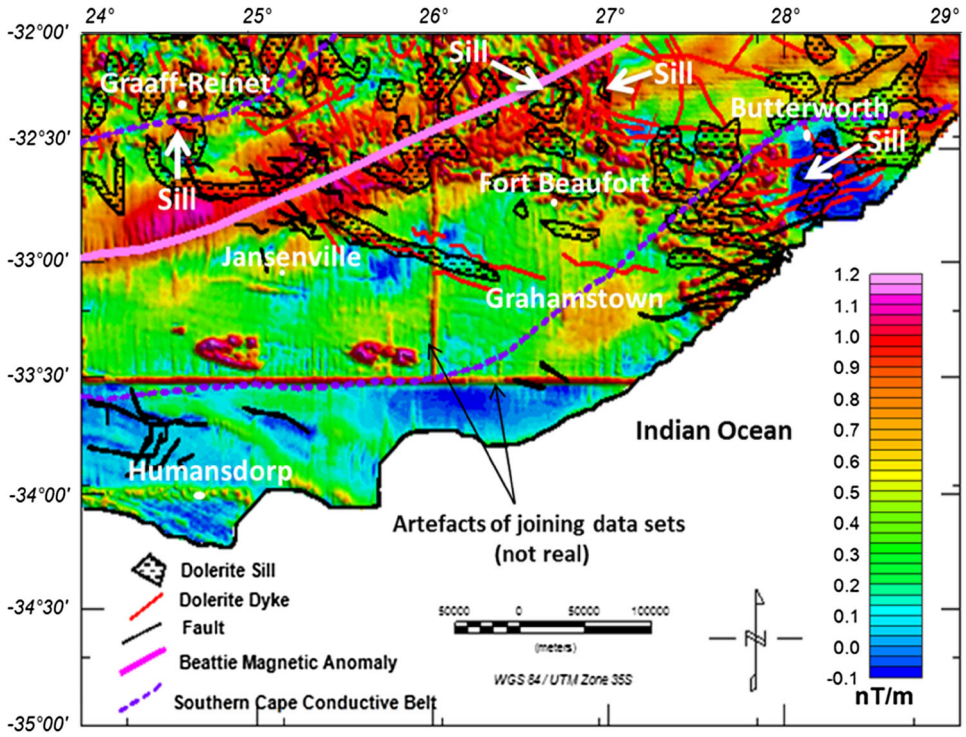

Fig. 11 Analytical signal magnetic map overlain on the geology

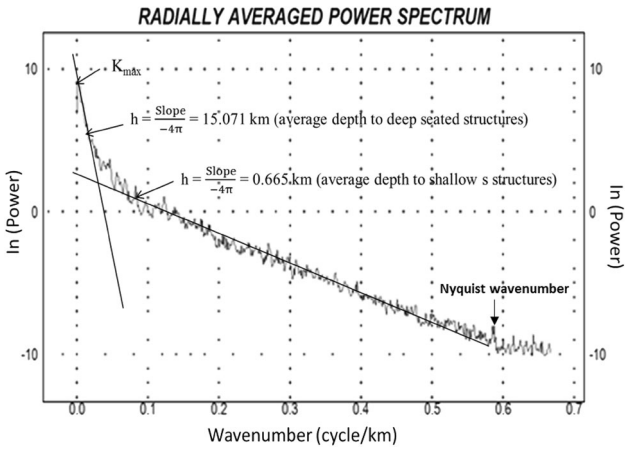

Fig. 12 Depth estimates from the radially averaged power spectrum

the geological map of the area. It shows that the mapped geologic structures such as dolerite intrusions have a response which is clearly visible down to a depth of about 3.3 km. The depths slice 4 (15.2 km) shows no anomalies due to intrusions when compared with the other slices (slice 1–3). A ring structure (inferred dolerite sill) seen in the northern part of the map becomes more prominent or stronger up to a depth of about 3.3 km, but thereafter it disappears at a depth of 15.2 km. The BMA appears in all the depth slices (0–15.2 km) and becomes broader and stronger up to a depth of 15.2 km. This could be an indication that the source is deeper, possibly within the basement. It could be a buried body in the basement. The bean shape anomaly (BSA) also behaves in a similar manner such as the BMA, so it could possibly have source(s) at similar depths to the BMA.

Gravity

The Bouguer gravity anomaly map (Fig. 14) shows an increase in gravity values from about −141 mGal inland (southwestern and northern side of Jansenville) to high gravity values of up to 62 mGal in coastal areas (western part of Humansdorp and continues to the northeast of Butterworth along the coastline). The dominant gravity highs seen along the coastal areas are of long wavelength. This is possibly due to a deeper source/interface inland that shallows southward towards the coast, e.g., the basement and/or Moho (this is seen on models presented in Figs. 15, 16, 17, 18).

Dry density

The calculated densities of the rock samples are listed in Table 3.

The average dry density for each geologic group falls within the range (2.3–2.8 g/cm^3) which is similar to the values obtained by several researchers, like Van der Voort (2001) and Johnson et al. (2006) that investigated the Karoo Basin in South Africa. The dry densities of rocks in the upper mantle (below the Moho) were extracted from literature (Hynes and Snyder 1995; Cook et al. 2010;

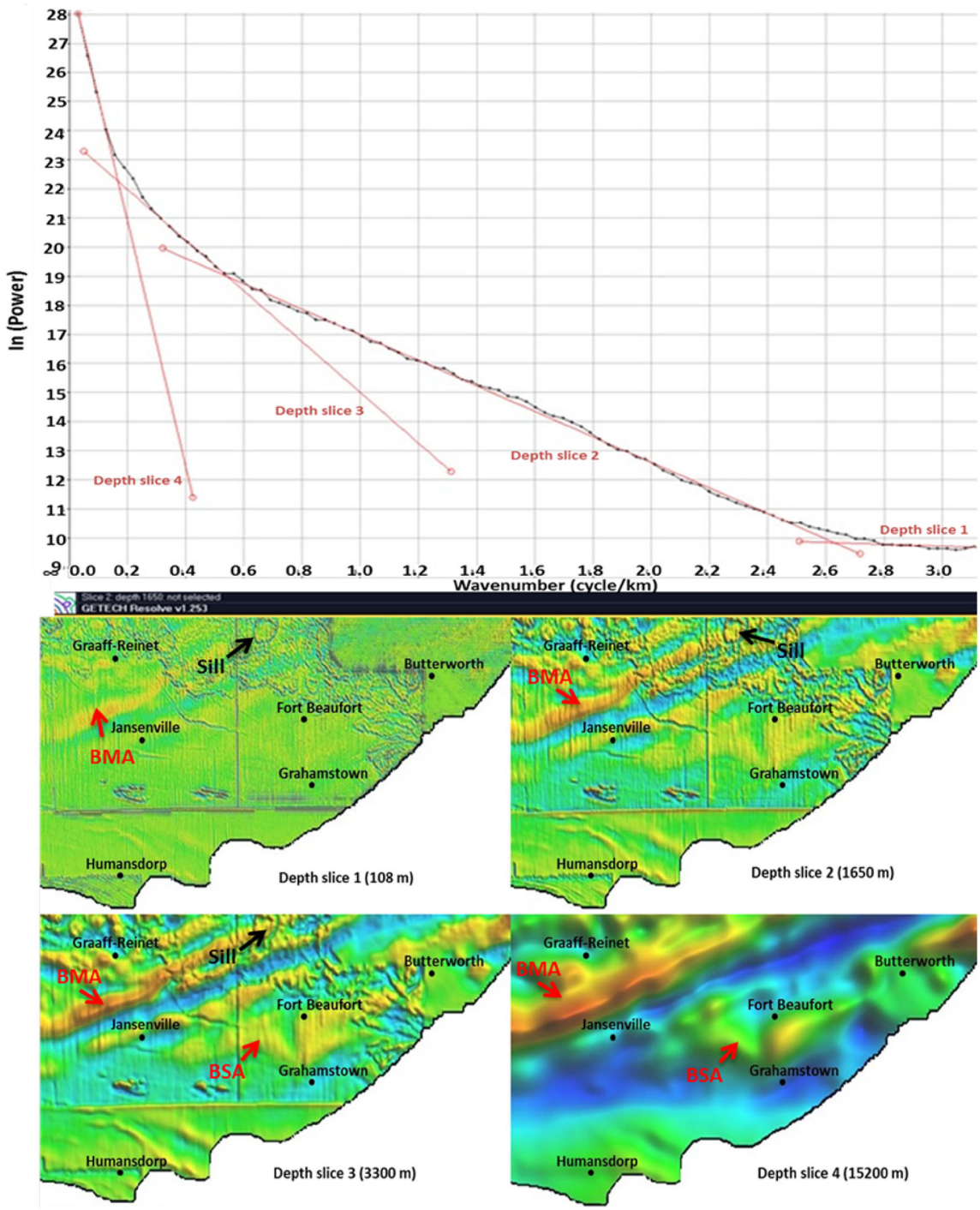

Fig. 13 Depth slice showing changes in anomaly features with depth. *Note* BMA is the Beattie Magnetic Anomaly and BSA is the bean shape anomaly

Mjelde et al. 2013; Thybo and Artemieva 2014) and the density values range from 3.14 to 3.4 g/cm^3.

½ D gravity profile models

The gravity modelling result of profile A–A′ is shown in Fig. 15. There is a relatively low gravity zone in the northwestern–southeastern part of the map, as shown along the profile. The minimum gravity value along this profile is about −190 mGal, whilst the maximum value is −24 mGal. The thickness of the Beaufort, Ecca and Dwyka Groups varies along this profile. The Karoo (Dwyka, Ecca, and Beaufort Groups) and Cape Supergroup (Witteberg, Bokkeveld, and Table Mountain Group) have

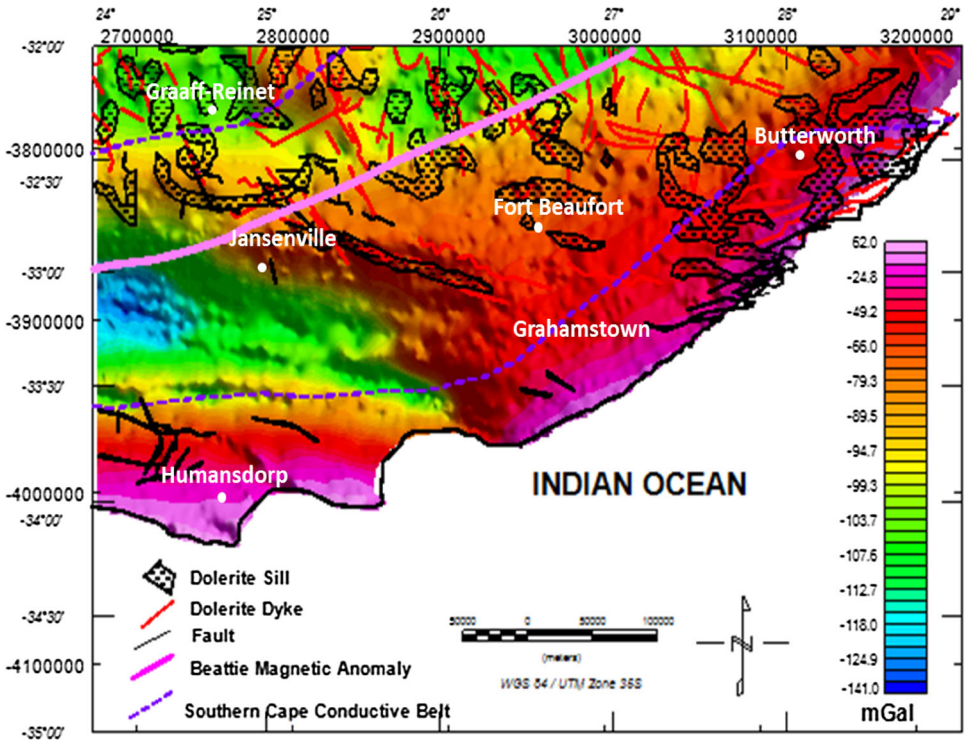

Fig. 14 Bouguer gravity anomaly map on the geology

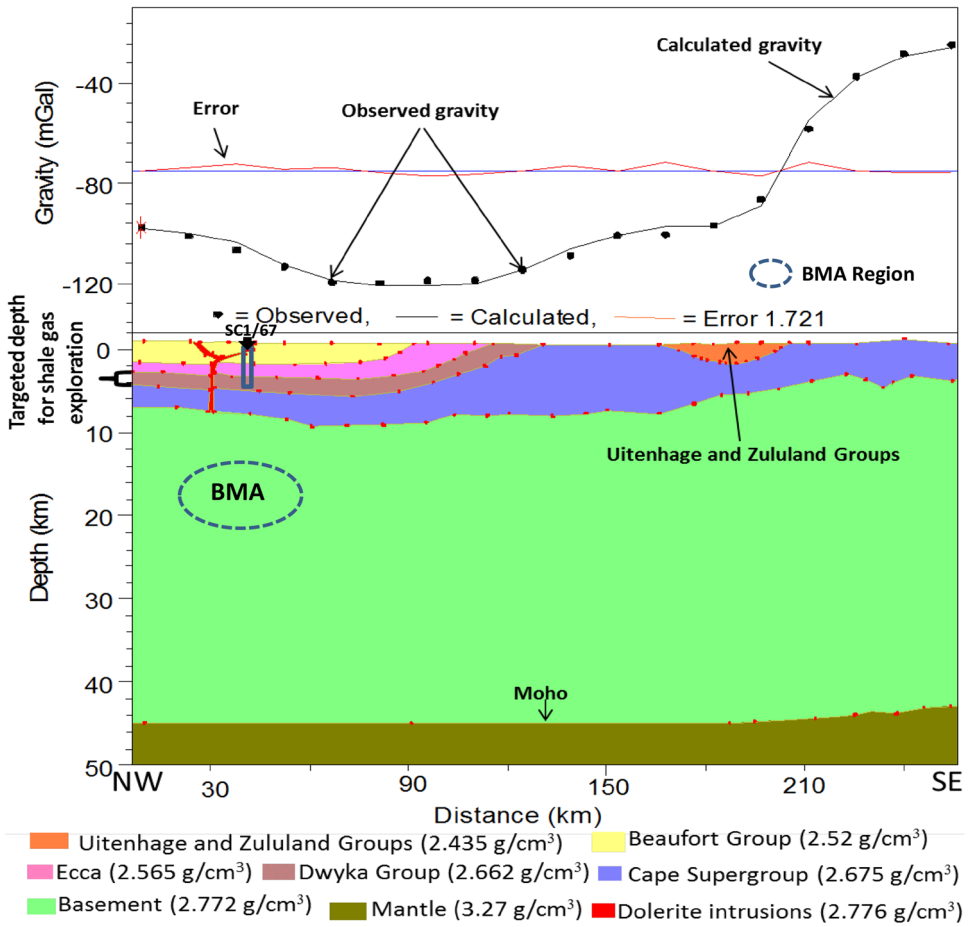

Fig. 15 Gravity modelling of profile A–A′. VE = 0.8; initial and final RMS errors are 64.4 and 1.7, respectively. Note: the shape of the BMA is unknown

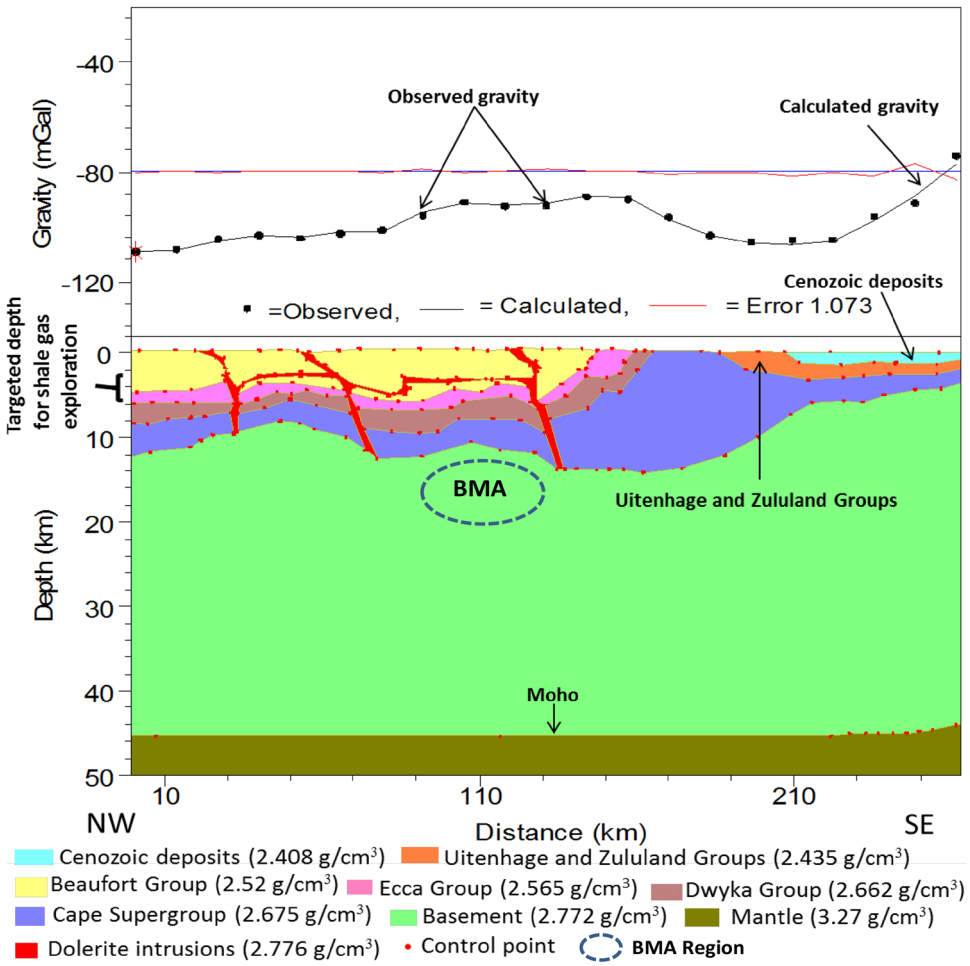

Fig. 16 Gravity modelling of profile B–B′. VE = 1.4; initial and final RMS errors are 110 and 1.2, respectively. Note: the shape of the BMA is unknown

been intruded by a dolerite dyke as shown in Fig. 15 which probably served as feeder to the sill that is seen in the Beaufort Group as well as outcropping on the surface. On the geology map, there are two places where dolerite intrusions are seen and these outcrops, as indicated in the model, merged at a depth of about 1.8 km. In addition, the Uitenhage and Zululand Groups (outcropping on the surface) are encountered along this profile between the distances of about 160–200 km, and they extend to about 1.8 km below the sea level.

The Bouguer gravity profile in Fig. 12 shows a remarkable gravity low towards the southeastern end of the profile (i.e., from 150 to 250 km). The layers in the model show undulations inferred to be due to deformation. In addition, the geologic sequence has been intruded by dolerites in the form of dykes and sills. The dykes probably served as feeders to the intrusions that outcrop on the surface. The Cenozoic deposits as well as the Uitenhage and Zululand Groups were seen along the profile (between the distance of 190 to about 240 km) and their thicknesses (i.e., up to 2.5 km thick) also varies across the profile. The surface expression (region) of the BMA along this profile is located between the distances of about 90–130 km. In the BMA region, there is no significant gravity anomaly noticeable on the profile. In addition, there is no significant departure of the Bouguer anomaly curve from the general background values that can be inferred to be due to the BMA. This could be an indication that the BMA has little or no density contrast with the basement.

The gravity model for profile C–C′ is shown in Fig. 17. The Bouguer gravity value increases steadily from the northwestern–southeastern direction of the map. The thickness of the Karoo (Beaufort, Ecca, and Dwyka) rand Cape Supergroup varies along this profile with noticeable undulations which may be due to deformation. The dolerite intrusions that outcrop on the surface are seen in the model extending to depth cutting through the Cape, Dwyka, Ecca, and Beaufort sequence in the form of dykes and sills (Fig. 17). Lateral displacement (faulting) is also seen cutting through the Cape, Dwyka, and Ecca Groups between distances of about 20 and 100 km. Along profile C–C′, the surface expression of the BMA is located between the distances of about 92–150 km. But again, the BMA does not have any appreciable gravity anomaly.

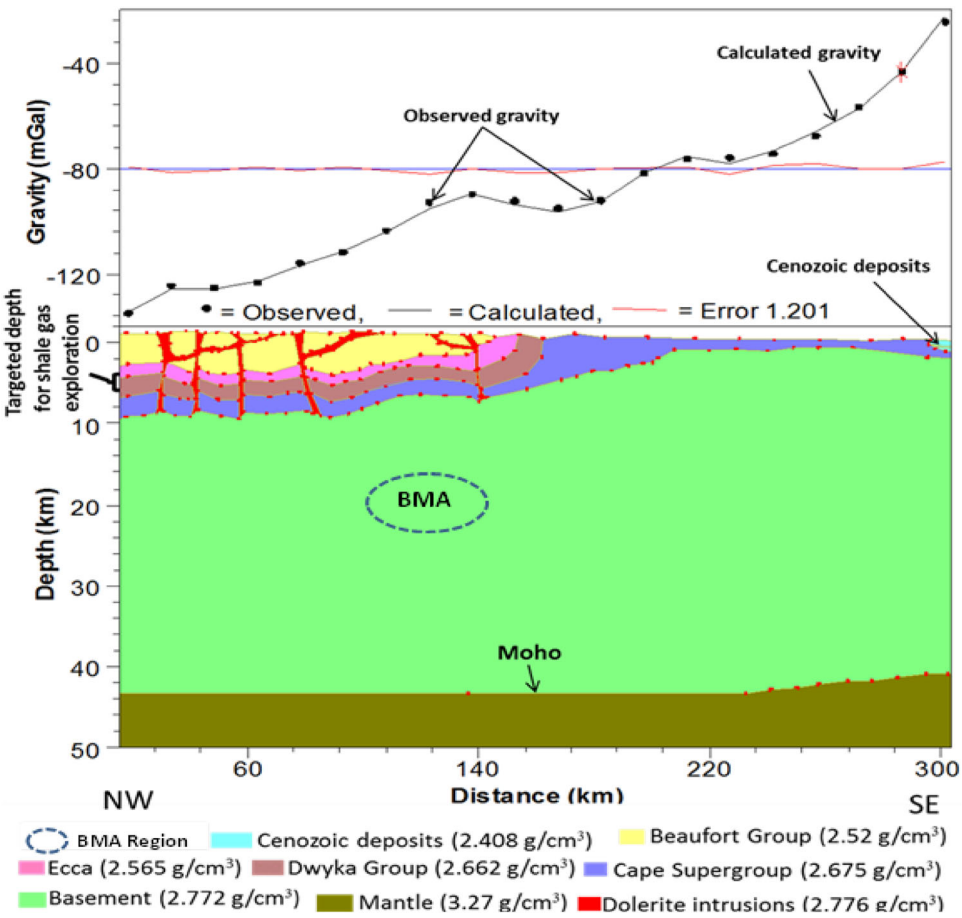

Fig. 17 Gravity modelling of profile C–C′. VE = 1.5; initial and final RMS errors are 65.4 and 1.2, respectively. Note: the shape of the BMA is unknown

Figure 18 shows model of profile D–D′. The minimum gravity value along this profile is about −136 mGal, whilst the maximum gravity value is −22.1 mGal. Generally, the thickness of the Karoo (Beaufort, Ecca, and Dwyka Groups) and Cape (Witteberg, Bokkeveld, and Table Mountain Groups) Supergroups varies along this profile probably due to deformation as depicted in the model by undulating surfaces. The geologic sequences have been intruded by dolerites that extend into the basement.

Discussion

In the study area, the total magnetic field residual anomalies increase from the coastal area to inland with three noticeable magnetic high zones (Fig. 6). The third magnetic zone which is part of the BMA split into narrow magnetic high zones as revealed by the vertical derivative map. The magnetic maps (Figs. 3, 4, 5, 6, 7, 8, 9, 10, 11) clearly show ring-like structures and lineaments which coincide with the mapped dolerite intrusions and some new ones are also revealed. The average magnetic depths of about 0.6 and 15 km were determined from the radially averaged power spectrum as the depths to the top of the shallow and deep sources, respectively. The BMA appears in all the depth slices and becomes broader and stronger up to a depth of 15.2 km. This could be an indication that the source(s) of the BMA is deeper possibly within the basement. Lindeque et al. (2007) documented that the BMA could be due to a buried body in the basement (that is possibly intersected by a fault plane dipping in a southern direction) or/and a buried massive sulphide-magnetite body within the basement. The average magnetic depths of about 15 km that was determined as the depths to the top of the deep sources could be linked to the BMA since the BMA appeared in all the presented depth slices. The estimated depth is also similar to the depth envisaged by Pitts et al. (1992) that the buried magnetic body of about 30 km width dips southward from about 7 km below the ground surface to a depth of up to 30 km. The BMA is one of the largest crustal anomalies in the world and trends northeast to southwest of the study area. It is suggested to be due to deeper source(s) possibly within the basement which agrees with the findings of Pitts et al. (1992) and Weckmann et al. (2007a). The bean shape anomaly also behaves in a similar manner such as the BMA, and thus it could possibly have a source(s) at similar depths to the BMA based on the depth slicing results.

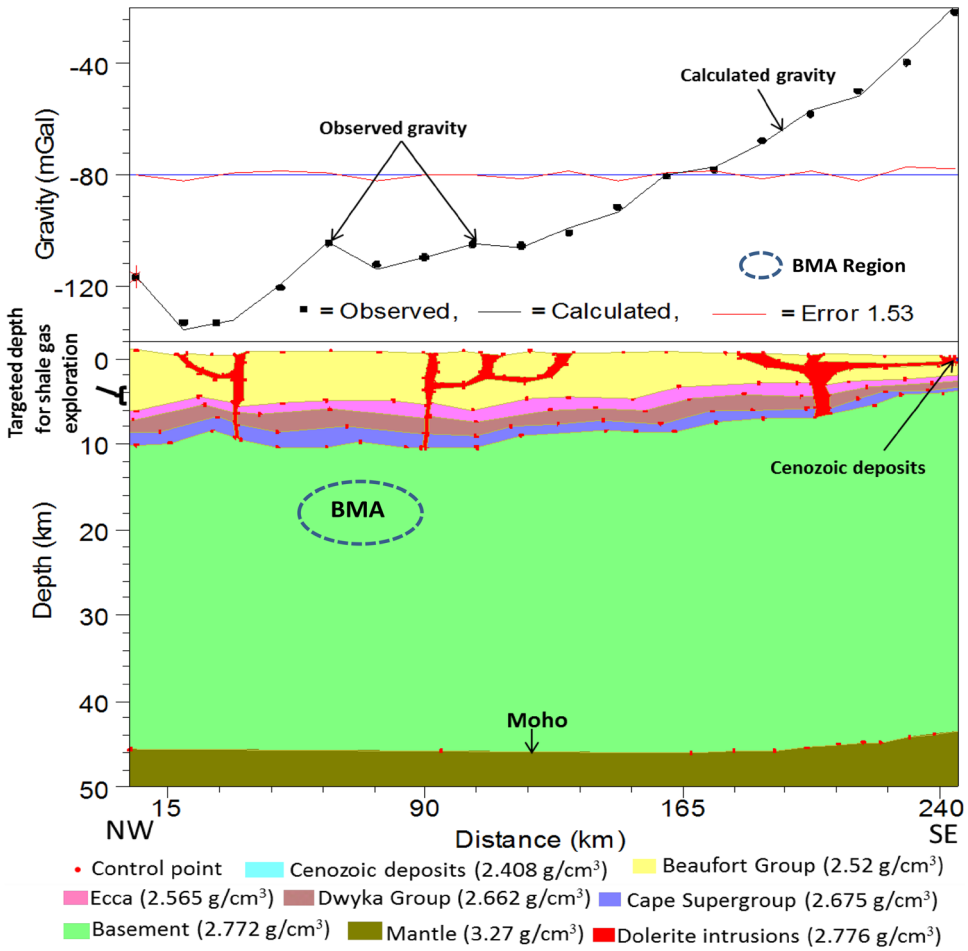

Fig. 18 Gravity modelling of profile D–D′. VE = 1.9; initial and final RMS errors are 48.3 and 1.5, respectively

Table 3 Rock density values used for gravity profile modelling

	Beaufort	Ecca	Dwyka	Cape	Dolerite intrusions	Basement or pre-cape	Below the Moho (mantle)
Lithology	Sandstone/mudstone	Mudstone	Diamictite	Sandstone/conglomerate	Dolerite	Chert/schist	–
No of samples	85	66	20	32	36	19	–
Highest density (g/cm^3)	2.77	2.78	2.68	2.72	2.83	2.82	3.40
Lowest density (g/cm^3)	2.27	2.35	2.59	2.63	2.71	2.72	3.14
Average density (g/cm^3)	2.52	2.57	2.66	2.68	2.77	2.77	3.27

The Bouguer gravity anomaly map (Fig. 14) shows an increase in gravity values from about −100 mGal inland to around 62 mGal in coastal areas. The 2½ D gravity profile modelling results show that the long wavelength variation is due to a deeper source/interface inland that shallows towards the coast, e.g., basement and/or Moho. Generally, the results of the modelling indicate a horizontal Moho at a depth of about 45 km inland and it shallows to about 42 km at the coastal area with a slope of about 3°. This shallowing of the Moho gives rise to the long wavelength gravity anomaly from inland to coastal areas. The Moho depth obtained in this study are in agreement with the depth results from Tedla et al. (2011) as well as Stankiewicz and de Wit (2013), which are in the range of 42–45 km for inland sections. The 2½ D gravity profile modelling results reveal a thickness of up to 8 km for the Karoo sedimentary sequence (i.e., depth from Beaufort to the Dwyka Group). The targeted area for shale gas exploration is the Ecca Group. All the four profiles cross the Ecca Group. Rowsell and De Swardt (1976) as well as Lindeque et al. (2011) have suggested a targeted exploration depth from about 3.5–5 km for shale gas and this depth range is within the

0–7.2 km determined from the gravity modelling. At the deepest section, the top of the Ecca Group is at 6.5 km depth and at the bottom is at 7.2 km. The determined laboratory dry densities range within about 2.59–2.68, 2.35–2.78, and 2.52–2.77 g/cm^3 for the Dwyka, Ecca, and Beaufort Group, respectively. The calculated porosities range within 0.29–0.87, 1.29–5.52, and 0.48–3.34% for the Dwyka, Ecca, and Beaufort Group, respectively. The high porosity and low density values of the Ecca samples could be possibly due to weathering. Based on the gravity profile models, the variation in thickness of the geologic units could be inferred to be due to deformation. In addition, it could be inferred that dolerite intrusions which are prominent in the study area are interconnected at depth as depicted in the models. This could possibly affect the quality of the shale resources and probably pose threat by increasing the risk of fracking the Karoo for shale gas exploration.

Conclusions

Based on the results presented in this paper, the following can be inferred:

- The anomaly which is part of the BMA tends to divide into two anomalies in the study area and continues to trend in an NE–SW direction. The BMA is possibly due to a source(s) buried deep, as shown by the depth slices.
- From the radially averaged power spectrum, the average depths to the top of the shallow and deep magnetic sources were estimated to be approximately 0.6 and 15 km, respectively.
- Based on the 2½ D gravity profile modelling and depth slice results, it could be deduced that geologic structures such as dolerite intrusions are interconnected and extend from the surface to a depth of about 12 km.
- The bean-shape anomaly, based on depth slice results, behaves in a similar manner, such as the BMA, and thus it could possibly have a source(s) at similar depth to the BMA.
- The dominant gravity signature in the coastal area is of long wavelength, which is possibly due to a deep source/interface inland that shallows towards the coast, e.g., basement and/or Moho. The Moho is at about 45 km depth inland and shallows to about 42 km at the coast.
- The 2½ D gravity profile modelling results reveal the configuration of the basin, with the Beaufort Group being the thickest (6342 ± 295 m) of all the groups that make up the Karoo Supergroup in the study area, followed by the Ecca (3207 ± 263 m) and Dwyka Groups (727 ± 25 m), respectively.

Acknowledgements Thanks to Govan Mbeki Research and Development Centre (GMRDC) for supervisory link bursary and NRF bursary to Mr C. Baiyegunhi (UID: 101980). The authors are grateful to Fugro Airborne Surveys, Council for Geoscience for supplying the geophysical data. Geosoft is also appreciated for providing the "Extended GM-SYS" that was used for the modelling. We thank the editors and anonymous reviewers for their constructive comments, which helped us to improve the manuscript.

References

Beattie JC (1909) Report of a magnetic survey of South Africa. R Soc Lond Publ 76:1–35

Catuneanu O, Hancox PJ, Rubidge BS (1998) Reciprocal flexural behaviour and contrasting stratigraphies: a new basin development model for the Karoo retroarc foreland system, South Africa. Basin Res 10:417–439. doi:10.1046/j.1365-2117.1998.00078.x

Catuneanu O, Hancox PJ, Cairncross B, Rubidge BS (2002) Foredeep submarine fans and forebulge deltas: orogenic off-loading in the underfilled Karoo Basin. J Afr Earth Sci 35:489–502. doi:10.1016/S0899-5362(02)00154-9

Catuneanu O, Wopfner H, Eriksson PG, Cairncross B, Rubidge BS, Smith RMH, Hancox PJ (2005) The Karoo basins of south-central Africa. J Afr Earth Sci 43:211–253. doi:10.1016/j.jafrearsci.2005.07.007

Chevallier L, Woodford AC (1999) Morpho-tectonics and mechanism of emplacement of the dolerite rings and sills of the western Karoo, South Africa. S Afr J Geol 102:43–54

Chevallier L, Goedhart M, Woodford AC (2001) The influences of dolerite sill and ring complexes on the occurrence of groundwater in Karoo fractured aquifers: a morpho-tectonic approach. Water Res Comm Rep 37(1):4–146

Cook FA, White DJ, Jones AG, Eaton DW, Hall J, Clowes RM (2010) How the crust meets the mantle: lithoprobe perspectives on the Mohorovicić discontinuity and crust–mantle transition. Can J Earth Sci 47:315–351. doi:10.1139/E09-076

Council for Geoscience (1995) Geological map of South Africa 1:250000, Sheet 2922, Prieska. Geological Survey of South Africa, Pretoria

De Beer JH, Gough DI (1980) Conductive structures in southernmost Africa: a magnetometer array study. Geophys J R Astron Soc 63:479–495. doi:10.1111/j.1365-246X.1980.tb02633.x

De Beer JH, Meyer R (1983) Geo-electrical and gravitational characteristics of the Namaqua–Natal mobile belt and its boundaries. Spec Publ Geol Soc S Afr 10:91–100

De Beer JH, Meyer R (1984) Geophysical characteristics of the Namaqua–Natal mobile belt and its boundaries, South Africa. J Geodyn 1:473–494. doi:10.1016/0264-3707(84)90020-6

De Beer JH, Van Zijl JSV, Gough DI (1982) The southern cape conductive belt (South Africa): its composition, origin and tectonic significance. Tectonophysics 83:205–225. doi:10.1016/0040-1951(82)90019-1

De Wit MJ, Horsfield B (2006) Inkaba yeAfrica Project surveys sector of Earth from core to space. EOS Trans Am Geophys Union 87(11):113–117. doi:10.1029/2006EO110002

De Wit MJ, Ransome IG (1992) Regional inversion tectonics along the southern margin of Gondwana. In: De Wit MJ, Ransome IG (eds) Inversion tectonics of the cape fold belt, Karoo and Cretaceous Basins of Southern Africa. Balkema, Rotterdam, pp 15–22

Du Plessis A, Simpson ESW (1974) Magnetic anomalies associated with the southeastern continental margin of South Africa. Mar Geophys Res 2:99–110. doi:10.1007/BF00340028

Flint SS, Hodgson DM, Sprague AR, Brunt RL, Van Der Merwe WC, Figueiredo J, Prélat A, Box D, Di Celma C, Kavanagh JP (2011) Depositional architecture and sequence stratigraphy of the Karoo basin floor to shelf edge succession, Laingsburg depocentre, South Africa. Mar Petrol Geol 28:658–674. doi:10.1016/j.marpetgeo.2010.06.008

Fuller BD (1967) Two-dimensional frequency analysis and design of grid operators. In: Hansen DA, Heinrichs WE, Holmer RC, MacDougall RE, Rogers GR, Sumner JS, Ward SH (eds) Society of exploration geophysicists' mining geophysics, vol 2. pp 658–708

Geel C, Schulz HM, Booth P, De Wit M, Horsfield B (2013) Shale gas characteristics of Permian black shales in South Africa: results from recent drilling in the Ecca Group (Eastern Cape). Energy Procedia 40:256–265. doi:10.1016/j.egypro.2013.08.030

Gough D, De Beer JH, Van Zijl J (1973) A magnetometer array study in southern Africa. Geophys J R Astron Soc 34:421–433. doi:10.1111/j.1365-246X.1973.tb02405.x

Gunn PJ (1972) Application of Wiener filters to transformations of gravity and magnetic data. Geophys Prospect 20:860–871. doi:10.1111/j.1365-2478.1972.tb00671.x

Hälbich IW (1983) A tectogenesis of the Cape Fold Belt (CFB). In: Söhnge APG, Hälbich IW (eds) Geodynamics of the Cape Fold Belt. Special publications of the geological society of South Africa, vol 12. pp 165–175

Hälbich IW (1993) The Cape Fold Belt—Agulhas Bank transect. In: Hälbich IW (ed) Cape Fold Belt—Agulhas Bank transect across Gondwana suture, Southern Africa. American Geophysical Union, Washington, pp 3–18. doi:10.1002/9781118668016.ch1

Harvey JD, De Wit MJ, Stankiewicz J, Doucouré CM (2001) Structural variations of the crust in the Southwest Cape, deduced from seismic receiver functions. S Afr J Geol 104:231–242. doi:10.2113/1040231

Hynes A, Snyder DB (1995) Deep-crustal mineral assemblages and potential for crustal rocks below the Moho in the Scottish Caledonides. Geophys J Int 123(2):323–339. doi:10.1111/j.1365-246X.1995.tb06857.x

Johnson MR, van Vuuren CJ, Hegenberger WF, Key R, Shoko U (1996) Stratigraphy of the Karoo Supergroup in southern Africa: an overview. J Afr Earth Sci 23:3–15. doi:10.1016/S0899-5362(96)00048-6

Johnson MR, van Vuuren CJ, Visser JNJ, Cole DI, Wickens HV, Christie ADM, Roberts DL, Brandl G (2006) Sedimentary rocks of the Karoo Supergroup. In: Johnson MR, Anhaeusser CR, Thomas RL (eds) The geology of South Africa. Geological Society of South Africa, Johannesburg/Council for Geoscience, Pretoria, pp 461–500

Li X (2006) Understanding 3D analytic signal amplitude. Geophysics 71(2):13–16. doi:10.1190/1.2184367

Lindeque A, Ryberg T, Weber M, Stankiewicz J, De Wit MJ (2007) Deep crustal seismic reflection experiment across the Southern Karoo basin, South Africa. S Afr J Geol 110:419–438. doi:10.2113/gssajg.110.2-3.419

Lindeque A, De Wit MJ, Ryberg T, Weber M, Chevallier L (2011) Deep crustal profile across the Southern Karoo basin and Beattie magnetic anomaly, South Africa: an integrated interpretation with tectonic implications. S Afr J Geol 114:265–292. doi:10.2113/gssajg.114.3-4.265

Maus S, Dimri V (1996) Depth estimation from the scaling power spectrum of potential fields. Geophys J Int 124(1):113–120. doi:10.1111/j.1365-246X.1996.tb06356.x

Mjelde R, Goncharov A, Müller RD (2013) The Moho: boundary above upper mantle peridotites or lower crustal eclogites, a global review and new interpretations for passive margins. Tectonophysics 609:636–650. doi:10.1016/j.tecto.2012.03.001

Pángaro F, Ramos VA (2012) Palaeozoic crustal blocks of onshore and offshore central Argentina: new pieces of the southwestern Gondwana collage and their role in the accretion of Patagonia and the evolution of Mesozoic south Atlantic sedimentary basins. Mar Petrol Geol 371:145–162. doi:10.1016/j.marpetgeo.2012.05.010

Pitts B, Mahler M, de Beer J, Gough D (1992) Interpretation of magnetic, gravity and magnetotelluric data across the Cape Fold Belt and Karoo Basin. In: De Wit M, Ransome I (eds) Inversion tectonics of the Cape Fold Belt, Karoo and Cretaceous basins of southern Africa. Balkema, Rotterdam, Netherlands, pp 27–32

Rabeh T, Abdallatif T, Mekkawi M, Khalil A, El-Emam A (2008) Magnetic data interpretation and depth estimation constraints: a correlative study on magnetometer and gradiometer data. NRIAG J Geophys Spec Issue 6:185–209

Rowsell DM, De Swardt AMJ (1976) Diagenesis in Cape and Karroo sediments, South Africa, and its bearing on their hydrocarbon potential. Trans Geol Soc S Afr 79:81–145

Rust IC (1973) The evolution of the Paleozoic Cape Basin, southern margin of Africa. In: Nairn AEM, Stehli FG (eds) The ocean basins and margins, vol 1, the South Atlantic. Springer, New York, pp 247–276. doi:10.1007/978-1-4684-3030-1_6

Scheiber-Enslin SE, Webb SJ, Ebbing J (2014) Geophysically plumbing the Main Karoo Basin, South Africa. S Afr J Geol 117(2):275–300. doi:10.2113/gssajg.117.2.275

Schreiber-Enslin S, Ebbing J, Eberle D, Webb S (2013) 3D Geophysical modelling of the Beattie magnetic anomaly and Karoo Basin, South Africa. Geophys Res Abstr 15:EGU2013-4407

Smith RMH, Erickson PG, Botha WJ (1993) A review of the stratigraphy and sedimentary environments of the Karoo-aged basins of Southern Africa. J Afr Earth Sci 132:143–169. doi:10.1016/0899-5362(93)90164-L

Spector A, Grant FS (1970) Statistical models for interpreting aeromagnetic data. Geophysics 35(2):293–302. doi:10.1190/1.1440092

Stankiewicz J, De Wit MJ (2013) 3.5 billion years of reshaped Moho, southern Africa. Tectonophysics 609:675–689. doi:10.1016/j.tecto.2013.08.033

Stankiewicz J, Ryberg T, Schulze A, Lindeque A, Weber MH, De Wit MJ (2007) Initial results from wide-angle seismic refraction lines in the Southern Cape. S Afr J Geol 110:407–418

Stollhofen H, Stanistreet IG, Bangert B, Grill H (2000) Tuffs, tectonism and glacially related sea-level changes, Carboniferous–Permian, southern Namibia. Palaeogeogr Palaeoclimatol Palaeoecol 161(1–2):127–150. doi:10.1016/S0031-0182(00)00120-6

Svensen H, Planke S, Chevallier L, Malthe-Sorenssen A, Corfu F, Jamtveit B (2007) Hydrothermal venting of greenhouse gases triggering Early Jurassic global warming. Earth Planet Sci Lett 256(3/4):554–566

Tankard AJ, Jackson MPA, Eriksson KA, Hobday DK, Hunter DR, Minter WEL (1982) Crustal evolution of Southern Africa. 3.8 billion years of earth history. Springer, New York, p 523

Tankard A, Welsink H, Aukes P, Newton R, Stettler E (2009) Tectonic evolution of the Cape and Karoo basins of South Africa. Mar Petrol Geol 26:1379–1412. doi:10.1016/j.marpetgeo.2009.01.022

Tankard A, Welsink H, Aukes P, Newton R, Stettler E (2012) Geodynamic interpretation of the Cape and the Karoo basins, South Africa. In: Regional geology and tectonics: phanerozoic passive margins, cratonic basins and global tectonics maps. Elsevier, pp 868–945. doi:10.1016/B978-0-444-56357-6.00022-6

Tedla GE, Van Der Meijde M, Nyblade AA, Van Der Meer FD (2011) A crustal thickness map of Africa derived from a global

gravity field model using Euler deconvolution. Geophys J Int 187:1–9. doi:10.1111/j.1365-246X.2011.05140.x

Thybo H, Artemieva IM (2014) Moho and magmatic underplating in continental lithosphere. Tectonophysics 609:605–619. doi:10.1016/j.tecto.2013.05.032

Turner BR (1999) Tectono-stratigraphical development of the upper Karoo foreland basin: orogenic unloading versus thermally-induced Gondwana rifting. J Afr Earth Sci 28:215–238. doi:10.1016/S0899-5362(99)00025-1

Van Der Voort I (2001), Risk based decision tool for managing and protecting groundwater resources. Ph.D. Thesis, University of the Free State, Bloemfontein

Veevers JJ, Cole DI, Cowan EJ (1994) Southern Africa: Karoo Basin and Cape Fold Belt. GSA Mem 184:223–280. doi:10.1130/MEM184-p223

Visser JNJ (1987) The palaeogeography of part of south-western Gondwana during the Permo-Carboniferous glaciation. Palaeogeogr Palaeoclimatol Palaeocol 61:205–219. doi:10.1016/0031-0182(87)90050-2

Visser JNJ (1995) Post-glacial Permian stratigraphy and geography of southern and central Africa: boundary conditions for climatic modelling. Palaeogeogr Palaeoclimatol Palaeocol 118:213–243. doi:10.1016/0031-0182(95)00008-3

Visser JNJ, Praekelt HE (1996) Subduction, mega-shear systems and Late Palaeozoic basin development in the African segment of Gondwana. Geol Rundsch 85:632–646. doi:10.1007/BF02440101

Weckmann U, Ritter O, Jung A, Branch T, De Wit M (2007a) Magnetotelluric measurements across the Beattie magnetic anomaly and the Southern Cape Conductive Belt, South Africa. J Geophys Res 112:416. doi:10.1029/2005JB003975

Weckmann U, Jung A, Branch T, Ritter O (2007b) Comparison of electrical conductivity structures and 2D magnetic modelling along two profiles crossing the Beattie Magnetic Anomaly, South Africa. S Afr J Geol 110:449–464. doi:10.2113/gssajg.110.2-3.449

Woodford AC, Chevallier LP (2002) Regional characterization and mapping of Karoo fractured aquifer systems—an integrated approach using a geographical information system and digital processing. Water Res Comm Rep 653/1/02:40–55